

HENRY

Hydraulic Engineering Repository

Ein Service der Bundesanstalt für Wasserbau

Conference Paper, Published Version

Kopmann, Rebekka

Simulation of embayment lab experiments using TELEMAC-3D/GAIA

Zur Verfügung gestellt in Kooperation mit/Provided in Cooperation with:
TELEMAC-MASCARET Core Group

Verfügbar unter/Available at: <https://hdl.handle.net/20.500.11970/110859>

Vorgeschlagene Zitierweise/Suggested citation:

Kopmann, Rebekka (2022): Simulation of embayment lab experiments using TELEMAC-3D/GAIA. In: Bourban, Sébastien E.; Pham, Chi Tuân; Tassi, Pablo; Argaud, Jean-Philippe; Fouquet, Thierry; El Kadi Abderrezzak, Kamal; Gonzales de Linares, Matthieu; Kopmann, Rebekka; Vidal Hurtado, Javier (Hg.): Proceedings of the XXVIIIth TELEMAC User Conference 18-19 October 2022. Paris-Saclay: EDF Direction Recherche et Développement. S. 215-221.

Standardnutzungsbedingungen/Terms of Use:

Die Dokumente in HENRY stehen unter der Creative Commons Lizenz CC BY 4.0, sofern keine abweichenden Nutzungsbedingungen getroffen wurden. Damit ist sowohl die kommerzielle Nutzung als auch das Teilen, die Weiterbearbeitung und Speicherung erlaubt. Das Verwenden und das Bearbeiten stehen unter der Bedingung der Namensnennung. Im Einzelfall kann eine restriktivere Lizenz gelten; dann gelten abweichend von den obigen Nutzungsbedingungen die in der dort genannten Lizenz gewährten Nutzungsrechte.

Documents in HENRY are made available under the Creative Commons License CC BY 4.0, if no other license is applicable. Under CC BY 4.0 commercial use and sharing, remixing, transforming, and building upon the material of the work is permitted. In some cases a different, more restrictive license may apply; if applicable the terms of the restrictive license will be binding.

Verwertungsrechte: Alle Rechte vorbehalten

Simulation of embayment lab experiments using TELEMAC-3D/GAIA

Rebekka Kopmann

rebekka.kopmann@baw.de, Karlsruhe, Germany
BAW

Abstract – One of the focal topics at BAW is the impact of river control structures such as groynes to optimise waterways maintenance strategies e.g. by means of sediment management. Hydro-morphodynamic numerical modelling supports the investigations of sediment management tasks. For inland river projects, sediment transport was usually considered as bedload only. For large-scale and long-term simulations, however, the exchange of suspended sediments between groyne fields and the main channel must be taken into account.

To investigate the numerical modelling capability of the lateral sediment exchange of non-cohesive material on inland waterways the laboratory experiment of [1] was chosen. Within this experiment the distribution of suspended sediment and its deposits in different configurations of lateral embayment were investigated. Using the two-dimensional approach of TELEMAC-2D/GAIA the numerical model could be calibrated to one discharge configuration but not validated to the other two discharges performed in the laboratory model [2], [3]. Therefore, further investigations were done with a higher resolution 2D model and with a three-dimensional model using TELEMAC-3D/GAIA.

The seiche effect of oscillating water levels found in the measurements could be reproduced by the high resolution 2D model. With the 3D model the centre of the embayment vortex was captured and the simulated deposition patterns could be improved. However, both models fail to reproduce the decrease in deposited material with increasing discharge.

Keywords: suspension, lateral sediment exchange, embayment.

I. INTRODUCTION

For inland river projects at BAW suspended sediment transport becomes more and more important. The requirements of the European Water Framework Directive cause investigations at the floodplains and the interaction between floodplain and main channel (e.g. the Federal program “Blaues Band Deutschland”). Within the BAW internal R&D project “Numerical modelling of lateral sediment exchange” the numerical modelling capability of the lateral sediment exchange of non-cohesive material on inland waterways is investigated. For long-term and large-scale studies the focus in the R&D project is on the lateral sediment exchange between groynes and main channel.

To validate the lateral sediment exchange, a laboratory experiment with lateral embayment was selected [1]. In this experiment the distribution of suspended sediment and its deposits in different configurations of lateral embayment were investigated. The simple geometry, the presence of concentration and deposition measurements and the excellent

description of the laboratory experiment seem to be good reasons to use this laboratory model as validation test case.

Using the two-dimensional approach of TELEMAC-2D/GAIA the numerical model could be calibrated to one discharge configuration but not validated to the other two discharges performed in the laboratory model [2], [3]. Especially the decrease in deposited material with increasing discharges could not be reproduced by the 2D model. Three possible causes were determined: the loss of material in the pores of the laboratory model, the embayment pumping effect, also known as seiche effect and a distinct three-dimensional flow in the shear zone between embayment and main channel.

It was assumed that the loss of material in the pores would not disturb the general trend of less deposition with higher discharges. Therefore, the two other possible reasons were followed for the configuration 3.1 of the experiment (see Figure 2).

The laboratory model is described briefly in chapter II. The applied numerical models are characterised in chapter III. In chapter IV the results of the numerical simulations are compared to the measurements with a focus to the deposition of sediment in the embayment areas.

II. EMBAYMENT FLUME EXPERIMENT

A 7.5 m long and 1 m wide flume with a longitudinal slope of 0.1 % were investigated by [1] (see Fig. 1). The experiments were done in a straight flume and four different embayment-length configurations. For this investigation configuration 3.1 was considered only (Fig. 2). In the experiment an artificial sediment of polyurethane corresponding to non-cohesive fine sediments were recirculated and mixed in upstream and downstream tanks. The measured main sediment parameters are a mean grain size of $d_{50} = 0.2$ mm, a density of 1160 g/m³ and a settling velocity of 0.00276 m/s.

Three different discharges (low flow: 4.8 l/s, medium flow: 8.5 l/s, high flow: 15 l/s) were conducted. The recirculating sediment mass which determines the boundary sediment concentration was found experimentally to the maximum suspended capacity of the flow for each discharge. It follows that no sediment deposited in the main channel.

The boundary conditions of the experiment are summarized in Table I. The concentrations or sediment masses were not measured at the boundaries. At two positions in the main channel orientated at the embayment configuration (see Fig. 1), turbidimeters were installed which monitored the concentrations. The vertical position of the turbidimeters was experimentally chosen to the vertical averaged value of the concentration profile. The averaged values of both measurement points are displayed in Fig. 3 for the reference configuration without embayment (3.0). The decrease in the concentration results from trapped sediments in small gaps between bricks and walls as in this configuration no bed evolution appeared. Furthermore, it was observed that the recirculating sediment procedure did not produce a constant feed but a decreasing, slightly oscillating one. The experiments were finished after 3, 4 and 5 hours when the bottom evolution in the lateral embayment were not measurable anymore. The concentrations reached a quasi-equilibrium concentration state for low, medium and high discharges, respectively (see Fig. 4 for configuration 3.1).

After the experiment the sediment mass trapped in the embayment was collected, dried and weighed. The total sediment mass divided by the total embayment area gives the trapping efficiency which is decreasing with increasing discharges (see Fig. 5).

The water level measurements show oscillations for all embayment configurations. The configuration 3.1 was one of those with the largest oscillations. This phenomenon is induced by a seiche, which occurs in dead zones of a flow (e.g. [4], [5]). Water level fluctuations of 1 – 3 mm were observed [1].

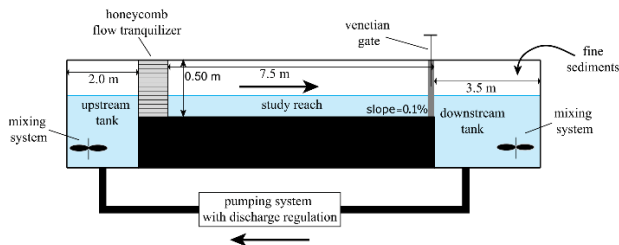


Figure 1: Side view of the set-up of the flume experiment (from [1]).

Table I Boundary conditions of the laboratory experiment.

Discharge (l/s)	4.8 (low)	8.5 (medium)	15 (high)
Water depth (m)	0.035	0.05	0.07
Recirculating sediment mass (kg)	2.75	5.5	8.25
Target sediment concentration (g/l)	0.5	1.0	1.5

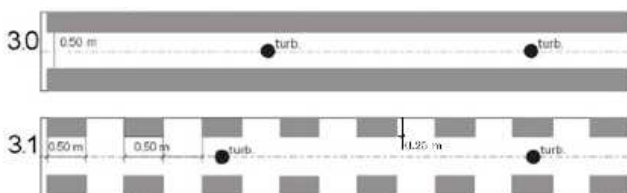


Figure 2: Embayment configuration 3.0 and 3.1 (from [1]).

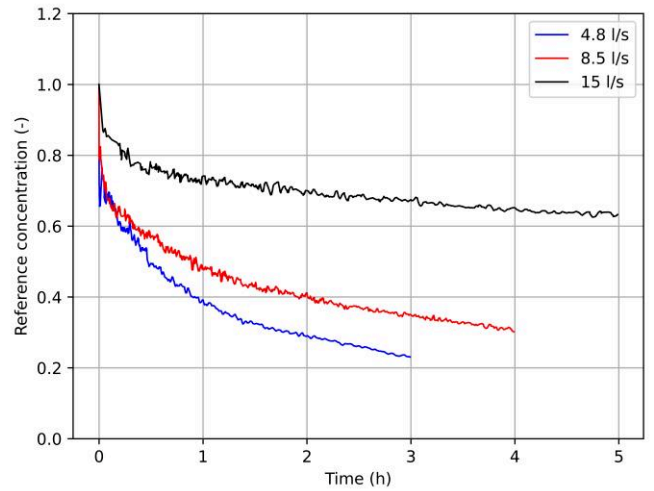


Figure 3: Measured concentrations for the configuration without embayment (3.0) (values are taken from [1]).

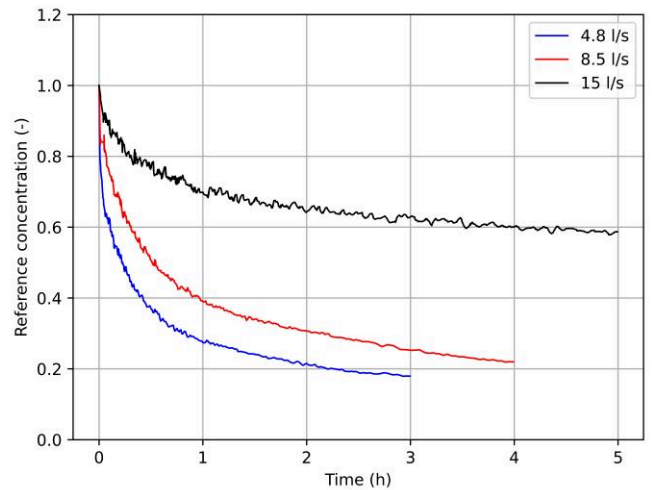


Figure 4: Measured concentration for configuration 3.1 (values are taken from [1]).

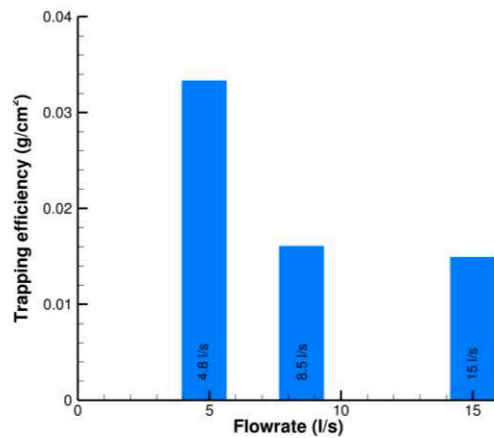


Figure 5: Measured trapping efficiency for configurations 3.1 and all discharges (values are taken from [1]).

III. NUMERICAL SIMULATION OF EMBAYMENT FLUME EXPERIMENT

Based on the numerical modelling of the laboratory experiment presented in [2] and [3] two new models were set up to improve the numerical results: A high resolution two-dimensional model (TELEMAC-2D/GAIA), denoted in the following as “2Dseiches”, was used to investigate the influence of seiches to the lateral sediment exchange. A moderate resolution three-dimensional model (TELEMAC-3D/GAIA), denoted in the following as “3Dcoarse”, was applied to resolve vertical processes. The “TUC2021” model is described in detail in [2] and is used in this paper for comparison. The new simulations were done for configuration 3.1 only. Table II shows the grid specifications of the different models. For stability reasons the inlet and outlet part without embayment areas are enlarged for the models 2Dseiches and 3Dcoarse.

The boundary conditions for the numerical modelling are summarised in Table III. At the inlet boundary the discharge and at the outlet boundary the water levels were imposed. For the TUC2021 simulations the horizontal velocity distribution at the inlet was set, taken from a previous steady state simulation. This procedure minimises the boundary impact but was not needed for the models 2Dseiches and 3Dcoarse due to the enlarged inlet. For the boundary sediment concentration at the inlet the averaged measurements along the channel (Fig. 4) were used.

Table II Applied models and their grid specifications.

Model name	Number of horizontal nodes	Number of horizontal elements	Number of vertical levels	Avg. horizon. node distance (m)	Avg. vertical node distance (m)	Time step (s)
TUC2021	2167	3872	1	0.05	-	0.05
2Dseiches	115067	224218	1	0.01	-	0.005
3Dcoarse	22838	42282	5	0.03	0.004 – 0.008	0.05

Table III Boundary conditions for the numerical models.

Discharge (l/s)	4.8 (low)	8.5 (medium)	15 (high)
Water depth (m)	0.035	0.05	0.07
Sediment concentration (g/l)	Measured concentration (see Fig. 3)		
Experiment duration (h)	3	4	5

TUC2021 simulations were started with steady state flow and concentration conditions found by a previous computation. No influence of this procedure to the trend of trapping masses with discharge could be found. Therefore, for the other models the initial velocities and concentrations were set to zero.

The roughness coefficients for the bottom (Nikuradse 0.5 mm) and for the lateral walls (Nikuradse 2.1 mm) were taken from the calibration of model TUC2021. For all models k-ε turbulence model was applied.

The sediment parameters were initially taken from TUC2021 but 2Dseiches and 3Dcoarse both consider sediment diffusion:

- Non-cohesive uniform grain size of 0.2 mm, porosity of 40%, density of 1160 g/m³, settling velocity of 0.00276 m/s
- Meyer-Peter Müller formula with factor 5 for bed load transport, slope effect (deviation: Talmon, magnitude: Soulsby), no secondary currents effect,
- adapted van Rijn reference concentration (20% of Nikuradse friction coefficient and between 1 and 20 % of water depth), including settling lag.

A. Model “2Dseiches”

The aim of the 2Dseiches model was to simulate the seiche effect in order to investigate the influence of the water oscillations on the trapping masses. With the numerical options of the TUC2021 model no seiches were simulated with the finer grid. Starting from the TELEMAC-2D validation example “cavity” the following options produce oscillating water levels:

- High resolution to minimise the numerical diffusion,
- no-slip boundary conditions for the embayments,
- Smagorinsky turbulence model,
- space discretisation with quasi-bubble.

For the space discretisation with quasi-bubble (DISCRETISATION IN SPACE = 12;11) the edge-based matrix storage (MATRIX STORAGE = 3) is required. This is not a default value in GAIA and must be set – otherwise the simulation will fail.

Some simulations were done with higher order schemes using finite volumes and higher resolution. The resulting oscillations are even higher and show more fluctuations laterally to the main flow direction while the finite element approach with quasi-bubble used here shows mainly fluctuations in the flow direction. Unfortunately, the higher order schemes did not run in coupled case with GAIA and were therefore not followed for this investigation.

B. Model “3Dcoarse”

In order to take three-dimensional effects into account the 3Dcoarse model was set up. The TUC2021 model could reproduce the embayment vortex but not completely at the correct position. Furthermore, the deposition areas did not fit very well to the measurements. Even a higher resolution of 1 cm node distances did not enhance these aspects [2].

Different horizontal and vertical resolution were tested. A relatively coarse resolution with 3 cm node distance in the horizontal and five vertical layers were chosen. Finer resolutions needed more computing time and showed some

strange effects if coupled to GAIA which could not be resolved.

Due to instability issues some changes / simplifications for GAIA needed to be done: no bedload transport, no settling lag but equilibrium concentration of van Rijn [6].

IV. COMPARISON OF THE NUMERICAL RESULTS TO THE MEASUREMENTS

A. Modelling of seiche effect

With the 2Dseiches model the measured water level oscillations could be simulated. In Fig. 6 the simulated free surface with coloured concentrations is visualised at half time of the experiment for all three discharges. In the centre of the left hand forth embayment (see marked probe position) the evolution of the water depth and concentrations over time are presented starting from the half time for 200 s. In [1] only the range of water level fluctuations were mentioned. Thus, the exact value for the experiment and the probe position is unknown. The probe position for the evaluation in Fig. 6 was chosen inside an embayment and with maximal distance to the open boundaries.

The simulated water level fluctuations are very much related to the probe position and vary from about 1 to 7 mm. Typically the oscillations are high in the shear zone and low in the embayment areas. In the main channel higher oscillations can be found in the narrow parts without lateral embayment areas. At the probe position water depth fluctuation of about 1 mm for 4.8 and 15 l/s and 2 mm for 8.5 l/s were found. This fits quite well to the measured 1 to 3 mm.

The concentrations at the probe position show also high frequent oscillations and additional a lower frequent disturbance. The high frequent amplitude increases with increasing discharge. The available concentration measurements are not precise enough for a useful comparison.

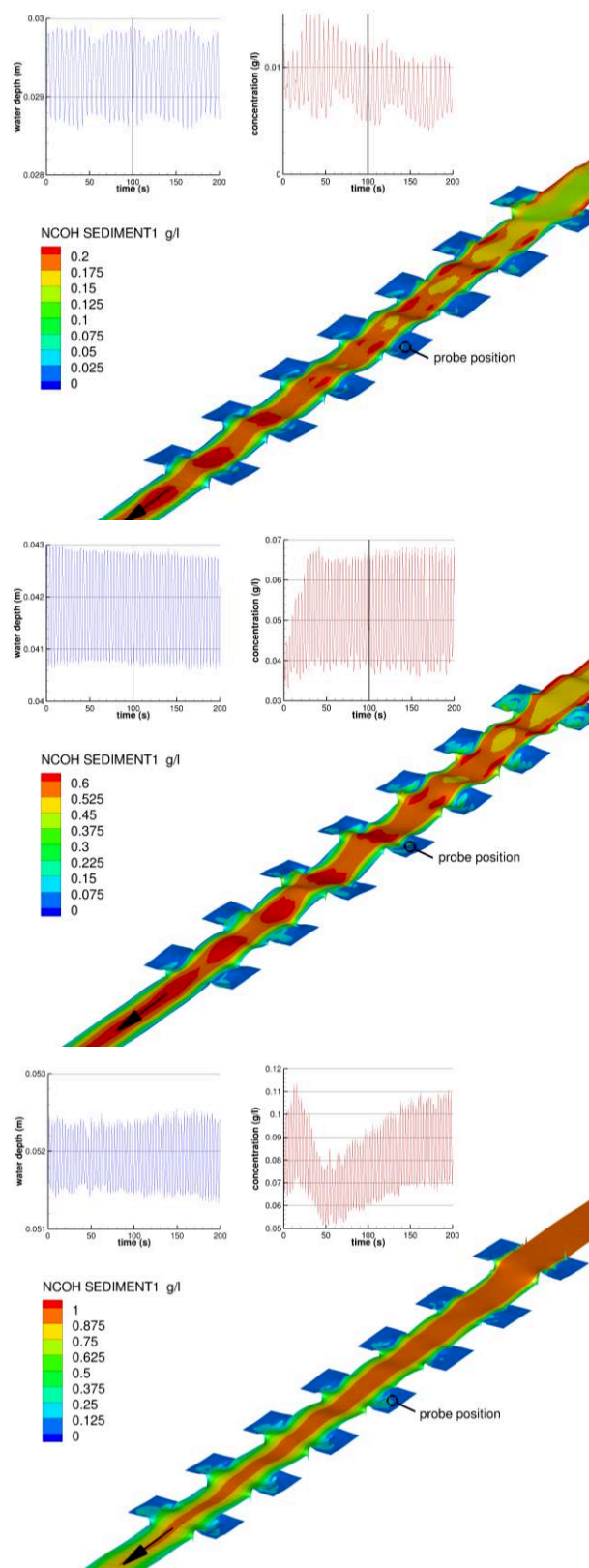


Figure 6: Oscillating water levels and depth averaged concentrations for a discharge of 4.8 l/s (top), 8.5 l/s (middle), 15 l/s (bottom) at half time of the experiment.

B. Modelling three-dimensional effects

Fig. 7 shows the simulated embayment vortex for all discharges in comparison to the measurements. Fig. 8 compares the embayment vortex for the TUC2021 model and the 3Dcoarse model for the high discharge. The three-dimensional simulations fit better to the measurements. The centre of the embayment vortex is at the dimensionless length parameter of the embayment $x/l \approx 0.7$ for the measurements and the 3Dcoarse model but at $x/l \approx 0.55$ for the TUC2021 model.

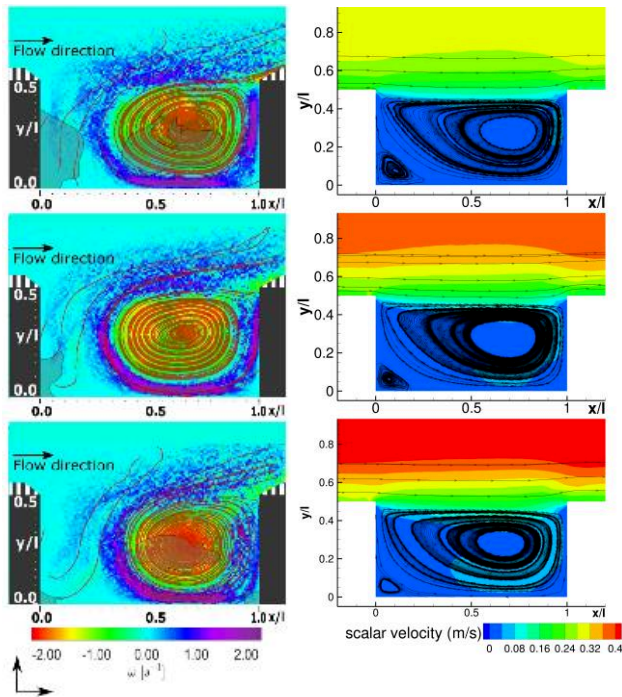


Figure 7: Comparison of measured vorticity and streamlines of the embayment vortex (left, from supplementary online data of [1]) and simulated scalar velocity and streamlines of the embayment vortex (right) for low (top), medium (middle) and high (bottom) discharges.

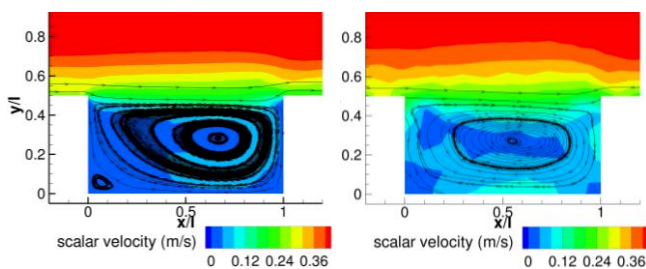


Figure 8: Comparison of simulated scalar velocity and streamlines of the embayment vortex for the 3Dcoarse model (left) and the TUC2021 model (right) for high discharge.

The simulated deposition pattern compared to the measurements is plotted in Fig. 9. As expected with three-dimensional simulation the material was deposited at the centre of the vortex. For the low discharge the lateral

exchange seems to be too small to transport the sediment through the shear zone. For this discharge the sediments deposited only along the shear zone. The measurements show for the low and the high discharge the typical deposition pattern in the centre of a vortex. Additionally, in the laboratory experiment deposition occurred mainly at the upstream corner. This effect could not be captured by the 3Dcoarse model although a second vortex was simulated in the upstream corner (see Fig. 8 left).

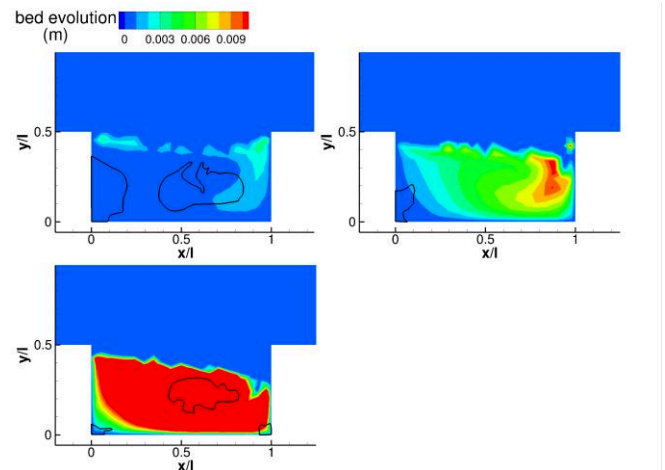


Figure 9: Simulated deposition for the 3Dcoarse model and position of measured deposition (black lines) for all discharges.

C. Comparison between simulated and measured trapping masses

The simulated deposited masses in the embayment areas are compared to the measured ones. In the experiment the deposition masses decreased with increasing discharges and increasing inlet concentrations. Fig. 10 presents the trapping efficiency over time for the models TUC2021, 2Dseiches, 3Dcoarse and the final value measured in the lab experiments.

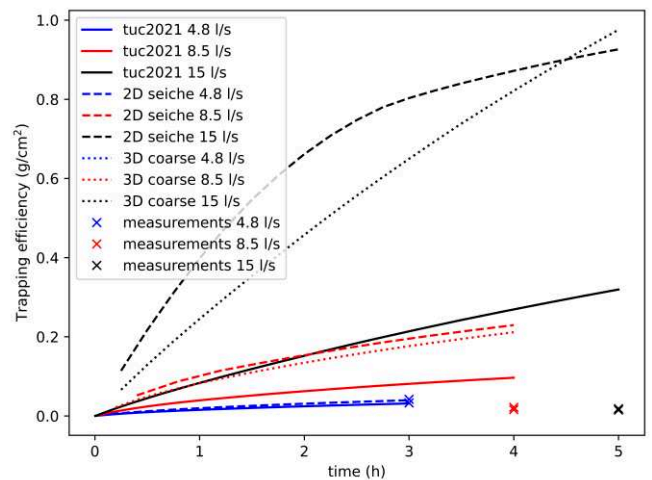


Figure 10: Trapping mass efficiency for the models TUC2021, 2Dseiches, 3Dcoarse and the measurements for all discharges.

For the small discharge the results of all numerical models fit very well to the measurements. But contrary to the measurements all models showed an increasing trend in deposition masses with increasing discharges respectively inlet concentrations. The increase was even higher for the more complex models. Both the seiche effect and the resolution of the vertical dimension led to a higher input of concentration into the embayment areas and a subsequent deposition.

The deposition of suspended sediments can be computed from the net sediment flux ($E - D$) as the result of the sedimentation (D) and erosion (E) processes. In GAIA the Sedimentation is calculated as product of the settling velocity w_s and the available concentration C_{zref} at a certain reference height $zref$. In 2D modelling a Stokes profile is assumed for the vertical distribution of the sediments. In 3D the simulated concentration at the reference height is used. The erosion for non-cohesive material is computed in GAIA as the product of the settling velocity and the equilibrium near-bed concentration C_{eq} , which is determined by an empirical formulation. For this investigation the formula of van Rijn was used which is dependent of sediment parameters, the reference height and the ratio between the Shields parameter and the critical Shields parameter.

$$E - D = w_s (C_{eq} - C_{zref}) \quad (1)$$

With increasing discharge, the inlet concentration in the experiment was increased, which led to higher concentrations in the embayment areas (see Fig. 6). The higher reference concentrations initiated higher sedimentation. It is assumed that the fluctuations also led to higher lateral sediment exchange, which increases the concentration inside the embayment areas, which in turn led to higher sedimentation. This would explain the higher trapping efficiency values for the 2Dseiche model compared to the TUC2021 model.

The 3Dcoarse model computed significantly smaller velocities (see Fig. 8) respective bottom shear stresses than the TUC2021 model (see Fig. 11). This caused smaller erosion which resulted in higher deposition tendencies. Fig. 11 shows the calculated Shields parameter of the TUC2021 and the 3Dcoarse model. GAIA computed a critical Shields parameter of 0.1. Therefore, erosion did not occur at dark blue parts. The 3Dcoarse model calculated much smaller Shields parameter than the 2Dseiche model because of the smaller flow velocities. For the 3Dcoarse model all sediments which were transported to the embayment areas were deposited with time. The linear increase for the trapping efficiency in Fig. 10 shows this.

For calibration purposes, the bottom shear stress was increased due to turbulence using the formulation proposed in [7]. This approach was already used within the TUC2021 model. Furthermore, the critical Shields parameter was reduced from 0.1 to 0.08 (after Soulsby & Whitehouse [8]). Both of these changes reduced the depositions for the higher discharges but did not change the general behaviour.

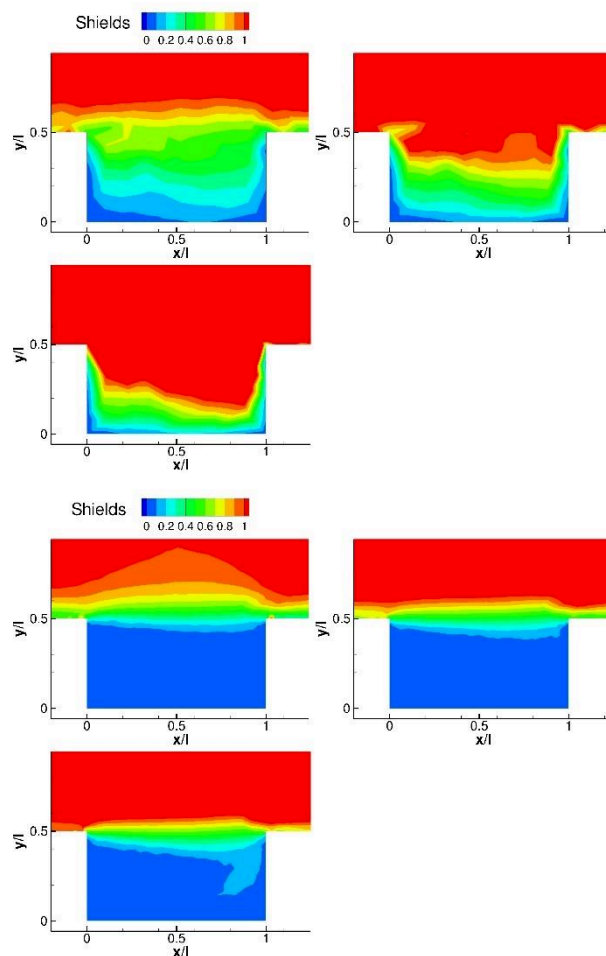


Figure 11: Comparison of simulated Shields parameter for the TUC2021 model (top) and the 3Dcoarse model (bottom) for all discharges.

V. CONCLUSION AND OUTLOOK

With the embayment experiment of [1] the capability of TELEMAC/GAIA to simulate lateral sediment exchange was investigated. Building upon the work of [2], [3] three different numerical models were compared to the experimental results in order to capture the measured decrease in trapped mass in the embayment areas with increasing discharge. Some shortcomings of the low resolution two-dimensional TUC2021 model could be overcome. With a high resolution 2D model (2Dseiches) it was possible to simulate the measured water level fluctuations. A three-dimensional approach (3Dcoarse) could also reproduce the centre of the embayment vortex and computed more reasonable evolution pattern in the vortex centre. But the deposition at the upstream corner of the embayment areas could not be reproduced.

All models considered could reproduce the trapping mass for the low discharge. Unfortunately, the decrease in the trapping mass with increasing discharges could not be simulated by any of them. The results of the new models were even worse probably due to the only rudimentary calibration. With increasing discharge and increasing inlet

concentration more sediment came into the embayment areas. So, the sediment deposition flux increased. For a smaller net sediment deposition, the erosion flux needed to be increased more than the deposition flux. But the bottom shear stresses increased only slightly and could not compensate the increased sediment flux.

It is assumed that the configuration of the laboratory experiment is quite special and probably related to a strong sensitivity of the light artificial material to turbulence. It seems that with higher discharges the sediments transported to the embayment areas did not settle but stay in the water column. In the literature, the effect of vortex trapping [9] is described. Sediment particles can move indefinitely along any circle in a forced vortex. It is unlikely that these special effects play a role in large-scale long-term lateral sediment exchange between main channel and groyne fields. Furthermore, the implemented formulas in GAIA were developed for natural sediments (sand) and produce not necessarily good results for artificial material and their sensitivities to turbulence. Therefore, the laboratory experiment seems not suitable as a validation test case for lateral sediment exchange of river groyne sections. Nevertheless, the investigations showed that even a low resolution 2D model (TUC2021) can be calibrated to catch the lateral sediment exchange.

The transferability to other discharges of emerged groynes could not be proven. Probably the long-term lateral sediment exchange is influenced mainly by the sequences between the flow of emerged and submerged groynes. Further investigations are planned including the validation on the basis of different laboratory experiments. One validation test case will be a new laboratory model with movable bed and bends conducted at BAW. Another could be a laboratory model with groynes [10].

ACKNOWLEDGEMENT

The author thanks Javier Obreque Perez for the fruitful collaboration and his work for this investigation.

REFERENCES

- [1] C. Juez, I. Bühlmann, G. Maechler, A. J. Schleiss, & M. J. Franca, Transport of suspended sediments under the influence of bank macro-roughness. *Earth Surface Processes and Landforms*, 43 (1), 271–284, 2018, <https://doi.org/10.1002/esp.4243>.
- [2] R. Kopmann, J. Perez-Obreque, Simulation of embayment lab experiments with TELEMAC-2D/GAIA. Proceedings of the TELEMAC-MASCARET User Conference October 2021.
- [3] J. I. Pérez Obreque, Modelling of lateral sediment exchange using TELEMAC2D/GAIA, Master thesis, Karlsruhe Institute of Technology, 2021
- [4] I. Kimura, T. Hosoda, Fundamental properties of flows in open channels with dead zone, *Journal of Hydraulic Engineering* 123: 98–107, 1997.
- [5] Y. Akutina, Experimental investigation of flow structures in a shallow embayment using 3D-PTV. PhD thesis, McGill University, Montreal, 2015.
- [6] L.C. van Rijn, Sediment transport - Part II : suspended load. *Journal of Hydraulic Division*, HY11:1631–1641, 1984.
- [7] A. Goll, 3D Numerical Modelling of Dune Formation and Dynamics in Inland Waterways. PhD thesis, Université Paris-Est, École du Pont ParisTech 2017, <https://hdl.handle.net/20.500.11970/104213>.
- [8] R.L. Soulsby, and R. J.S. W Whitehouse. Threshold of sediment motion in coastal environments. In, Proceedings Pacific Coasts and Ports '97 Conference, 1, 149154. New Zealand: Christchurch, University of Canterbury, 1997
- [9] P.F. Tooby, G. L. Wick, and J. D. Isaacs, The motion of a small sphere in a rotating velocity field: A possible mechanism for suspending particles in turbulence, *J. Geophys. Res.*, 82(15), 2096–2100, 1977.
- [10] Mohamed F. M. Yossef and Huib J. de Vriend, Sediment Exchange between a River and Its Groyne Fields, Mobile-Bed Experiment, *Journal of Hydraulic Engineering*, 136(9), 610–625, 2010 [https://doi.org/10.1061/\(ASCE\)HY.1943-7900.0000226](https://doi.org/10.1061/(ASCE)HY.1943-7900.0000226).